# 6.7 Lidar Global Cloud and Aerosol Layer Distribution Statistics from GLAS Observations

William D. Hart*, Stephen P. Palm, and Dennis L. Hlavka
Science Systems and Applications Inc., Lanham, MD

James D. Spinhirne
NASA Goddard Space Flight Center/912, Greenbelt, MD

## 1. INTRODUCTION

Clouds induce a crucial modulation of terrestrial shortwave reflectivity and longwave absorptivity and emissivity. Therefore, knowledge of the global distribution of cloud cover is essential in understanding the radiative budget of the earth and its atmosphere. Detection of trends and variations in the global climate require firm knowledge of the radiation budget.

For several decades, routine observations of global cloud distributions have been made with passive radiometers on operational meteorological and earth observation satellites. Some examples are the High resolution Infrared Radiation Sounder (HIRS) and Advanced Very High Resolution Radiometer (AVHRR) mounted on NOAA satellites, TIROS Operational Vertical Sounder (TOVS) aboard TIROS satellites, and the Moderate Resolution Imaging Spectroradiometer (MODIS) aboard the Terra (EOS AM) and Aqua (EOS PM) satellites. While providing continuous and widespread coverage of global cloud distribution, radiometer observations generally lack sensitivity to optically thin clouds and produce ambiguous results in discerning multiple cloud layers.

As an active remote sensing device, the Geoscience Laser Altimeter System (GLAS), launched into orbit in January, 2003 aboard the freeflying Ice, Cloud, and Land Elevation Satellite (ICESAT), provides a means to improve the results of the observations made by radiometers and to evaluate their results. GLAS is a dual-purpose laser instrument, serving both as a precision surface elevation altimeter and atmospheric lidar. Initially intended to provide continuous observations for a 3-5 year time span, technical problems have significantly truncated the its useful lifetime and have forced GLAS to be operated during discreet time intervals. Nevertheless, during its periods of operation, GLAS provides continuous and nearly pole-to-pole atmospheric lidar observations of the global cloud pattern. As a lidar, GLAS is sensitive to optically rarified atmospheric layers and is capable of detecting multiple layers if the higher layers are optically thin. This capability can provide certain insight to radiometer results when comparisons are made.

The routine GLAS product sets include cloud and aerosol layer heights and layer optical depths. We have used these products to garner statistical characterizations of global cloud and aerosol layer occurrence distributions, multiple layer distributions, layer altitudes, and layer optical depths. In this presentation, we show the results of some of these characterizations. In our presentation, we show histograms of occurrences of clear skies and single and multiple layers on a global basis and as a function of region. We show global and regional mapping of average cloud top heights. We show results of statistical studies designed to address limits of sampling requirements for meaningful results. Comparisons with results from satellite radiometer studies are made. Similar statistics from different times and places are compared and contrasted to detect potential trends and geographic variations. We demonstrate the observations from GLAS and other future spaceborne lidar significantly enhance knowledge of the global distribution atmospheric layers.

## 2. LAYER DETECTION

Details of the GLAS lidar system are given in the Algorithm Theoretical Basis Document (ATBD, Palm *et* all, 2001). Briefly, it is an elastic backscatter system with channels at 1064 nm and 532 nm. The system produces 40

---

*Corresponding author address: William D. Hart, Code 912, NASA/GSFC, 8800 Greenbelt Rd. Greenbelt, MD 20771
email: billhart@agnes.gsfc.nasa.gov

atmospheric profiles per second with at 76 m vertical resolution.

The GLAS cloud-layer detection algorithm is a single-pass threshold comparison technique designed for use with 532 nm data. For the purpose of our analysis, a time series of GLAS profiles is divided into four-second segments. An averaged attenuated backscatter coefficient profile is computed for a selected time segment. A corresponding threshold profile is fabricated from computed Rayleigh backscatter values and the vertical variability of the observed profile. Layers are found by comparing the backscatter coefficient profile with the threshold profile in a top to bottom sequence. If a specified number of consecutive bins exceed the threshold, a cloud top is assigned to that position. A layer bottom is assigned to where the signal magnitude of a number of consecutive bins falls below the threshold value. Cloud layers are distinguished from aerosol layers by using a parameter based upon the product GLAS signal magnitude and gradient of magnitude.

In order to reduce the influence of random noise on layer detection, the GLAS algorithm uses a cascading procedure for layer detection. After cloud layers have been have been found at four second resolution, equivalent searches are done at 1 second and 0.2 second resolutions. Layers found at these resolutions are accepted only if layers have been found at the same altitude at the coarser resolutions. A sample GLAS cloud layer detection for a 5Hz profile is shown in Figure 1. This example illustrates that a quite tenuous cloud signal can be found in a noisy profile. Layer detection results for a data segment are shown in Fig. 2. A more complete description of this algorithm can be found in Palm *et al.*, 2001.

Layers detected at 0.2 second resolution (5Hz) are used in the analysis presented herein. Averages and observational occurrence frequencies for a time range are computed from all observations in a defined geographical region. Temporally contiguous observations are not truly independent but the effect of this is mitigated with a long observation period.

## 3. DATA ANALYSIS AND RESULTS

Fractional cloud cover, cloud altitude, and multiple layer information are important characteristics that can be determined from satellite observations. In general, passive radiometric observations made from satellites can reliably detect the presence of cloud cover in a grid cell but they do not dependably find accurate cloud altitude or presence of multiple layers. Radiometric techniques rely on measurements of integrated signal at multiple wavelengths that require assumptions about reflective and emissive background and the thermal structure of the atmosphere. Since lidar is a ranging device, it can determine cloud

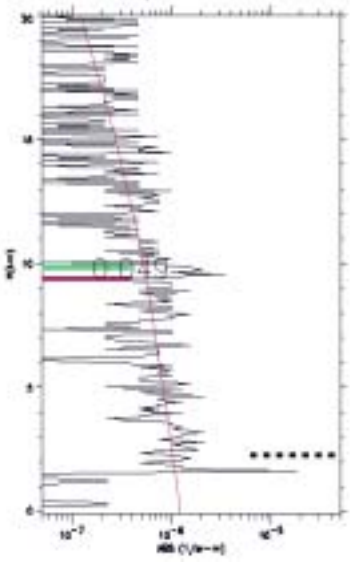

**Figure 1.** Sample layer boundary detection for 5Hz GLAS profile (black line) . Green horizontal line indicates analyzed top, red line is bottom, and red vertical line is computed Rayleigh. Numeric value is computed optical depth.

altitudes very accurately. Typically, GLAS finds locates significant cloud layers to within about +/- 76 m. Since cloud detection with lidar is not very sensitive to vertical temperature structure, detailed knowledge of the atmospheric thermal distribution is not required The implication of this is that lidar results can be used to evaluate

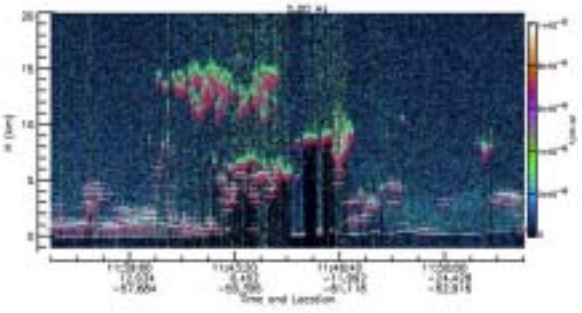

**Figure 2.** Sample layer boundary detection at 5Hz. Top of layers are in green, bottoms are in red. Small crosses indicate cloud layers and large crosses are aerosols

results obtained with passive instruments. In finding occurrences of multiple layers, GLAS observations are limited to a total optical depth of about 3. Any layer underneath that level cannot be detected by GLAS

As mentioned previously, GLAS data have been taken only during a limited number of time segments Of those, the time period 16 Oct. 2003 to 15 Nov. 2003 is the time segment when 532 nm data best for analysis were taken. Because the sampling period is limited to a single month, comparisons with other satellite observation can result in only qualified conclusions.

A depiction of the total global cloud cover during this period is shown Figure 3. The most important information found here is that GLAS is detecting very close to a 70% global cloud cover for combined day and night observations for all cloud altitudes. As a comparison, Wylie *et. al.*, 1994, report an average total global cloud cover of 76.8% based upon four years of HIRS observations. Also, a single cloud layer is detected in about 45% of the observations, which include multiple layer situations that are missed because of large optical depth of the first layer. Where layers are detected, GLAS detects multiple layers in about 40% of the cases. This result has implications for algorithms used for passive observations that make an assumption of a single cloud.

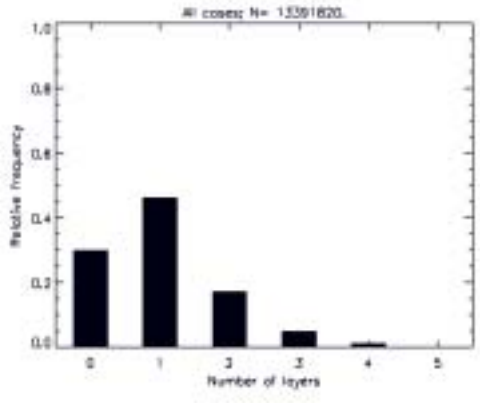


**Figure 3.** Global cloud layer occurrence found by GLAS during 16 Oct. 03 through 15 Nov. 03.

GLAS cloud layer occurrence results by latitude zones are shown in Fig. 4. Several prominent features are noticeable in frequency of cloudiness depicted by the green line. The equatorial region shows a local maximum of cloudiness, presumably associated with the Intertropical Convergence Zone (ITCZ). Contrasting to that are the local minimums of cloudiness at about S30 degrees and N30 degrees of latitude. These can be attributed to the general global scale subsidence associated

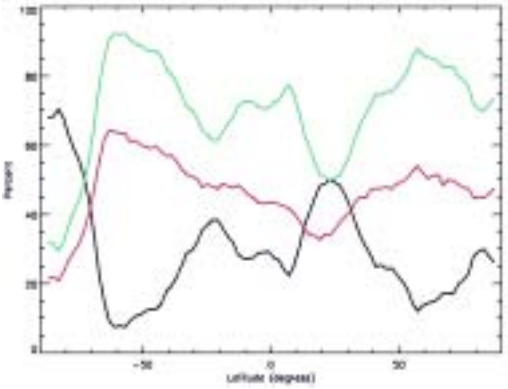

**Figure 4.** Meridional occurrence of clear (black), cloudy (green), and one layer only (red) GLAS observations between 16Oct. 04 and 15 Nov. 04

with Hadley cell circulation. The features have somewhat greater amplitude in the Northern Hemisphere, possibly because the time period is the transition from northern summer. Both hemispheres show maximum cloudiness in the temperate regions immediately adjacent to the polar region, reflecting the global scale ascension associated with Ferrel cell circulation. In the polar regions, the cloudiness decreases toward the poles except for a small increase closest to the pole. The plot demonstrates a significant qualitative hemispheric symmetry about the central tropical region.

Cloud top altitude is an attribute of much importance to climate evaluation. Satellite observations of clouds using passive radiometers attempt to determine cloud top heights. The ranging capability of lidar observations permits reliable and accurate determination of cloud altitude for single layer and multiple layers in cases of high layers with small optical depth. Fig. 5 shows the zonal average of cloud layer top as a function of latitude. The prominent features are the maximum altitude over the equatorial region, the local minimum in the Hadley cell subsidence region. the decease in altitude as a function of distance from the equator in the middle and high latitudes, which is the result of the decrease in the height of the tropopause. The increase in average height in the south polar region results a persistent deep layer near the pole With a lidar operating continuously for a period of years,

these types of observations could be monitored for temporal trends that may be caused by global climate change. This would be a very valuable and unique contribution of satellite lidar.

We see in Fig. 6. a worldwide depiction of the frequency of cloud cover. Cloudiness is found in expected latitudinal bands as was discussed for Fig. 4. Variation as a function of longitude is seen. The land masses are, on the average, less cloudy than ocean areas. The most uniformly cloudy latitude band is in the southern

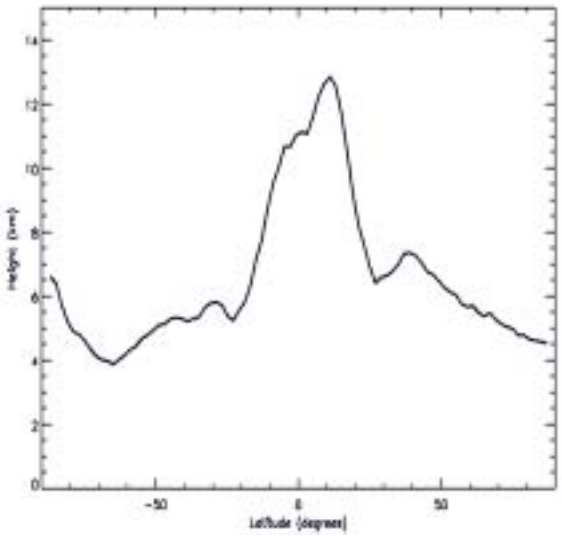

**Figure 5.** Zonal average cloud top height for GLAS observations between 16Oct. and 15 Nov. 2003

Hemisphere between S50 and S70 degrees. We also see an abrupt discontinuity in cloudiness at the edge of the Antarctic continent. This results from the transition from low level oceanic cloudiness to high continental plateau where that type of cloud is less likely.

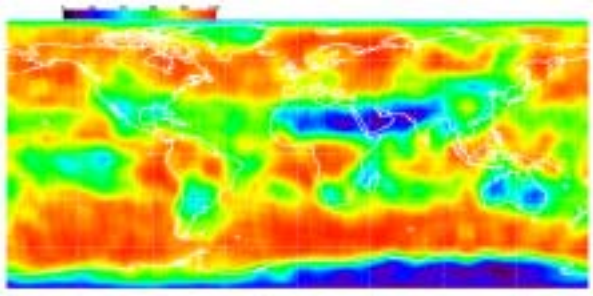

**Figure 6.** Frequency of cloudiness (percent) for GLAS observations between 16 Oct. and 15 Nov. 2003. The frequencies are for 1x1 degree lat/lon cells.

In Fig. 7 we show average cloud top for all clouds observed during the observation period in a 1x1 degree latitude/longitude grid. Among many interesting features are the minimums found just off the west coasts of South America, Africa, Australia, and North America. These probably result from persistent stratocumulus layers that are associated cold ocean surface layers found in these regions. Another obvious

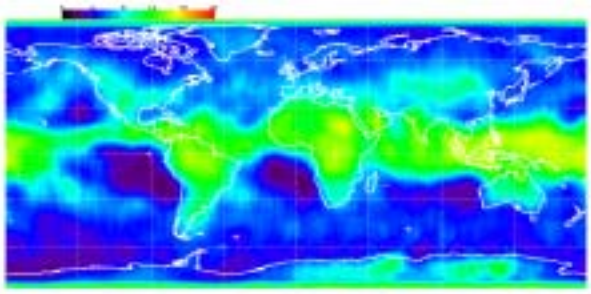

**Figure 7.** Average cloud top height (km,MSL) for GLAS observations between 16Oct. and 15 Nov. 2003. The averages were computed in 1x1 degree latitude/longitude cells.

characteristic is the very high average cloud top band caused by the deep convection encircling equatorial earth. Highest average cloud tops are found in the warm pool region in the equatorial western Pacific ocean region.

To illustrate a qualitative comparison of GLAS results to satellite results, Figures 8 and 9 show results obtained by MODIS in the October-November 2003 time period (see acknowledgement). The MODIS data product

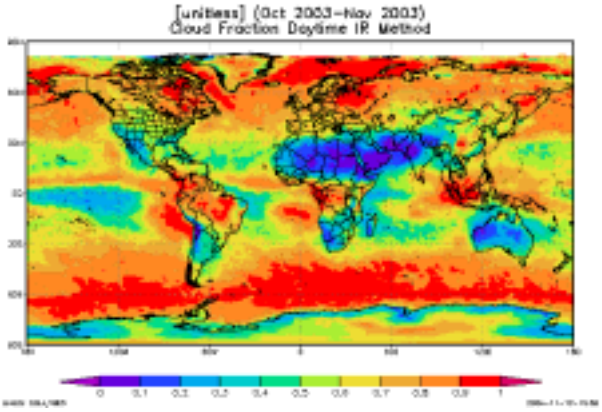


**Figure 8.** Frequency of cloudiness (percent) for MODIS observations, October and November. 2003; daytime IR method.

images were selectable only by calendar months, so a two month time span is used. Also, the average cloud tops are given in pressure and cloud occurrence frequency is for daytime observations only. Nevertheless, certain comparisons and contrasts can be made. Fig. 8 shows the same general global scale features as were depicted in Fig. 6 for the GLAS observations. A fine detail such as the cloudiness minimums found in eastern and western Australia is seen in both displays. A difference between the two is seen in eastern hemisphere Antarctica, where GLAS shows a minimum, is possibly caused by a bias in GLAS cloud/aerosol classification that existed when the GLAS product was made. The effect of the bias is reduced in subsequent versions of the product

A MODIS average cloud top pressure map in shown in Fig. 9 to compare with GLAS cloud top results show in Fig. 7. Both displays show low stratocumulus cloud tops off the west coasts South America, African, Australia, and North America. And as expected, high altitude cloud tops are found in tropical regions with the highest occurring in the western Pacific ocean. Finally, both displays show higher cloud tops in the Eastern hemisphere of Antarctica than in the western hemisphere.

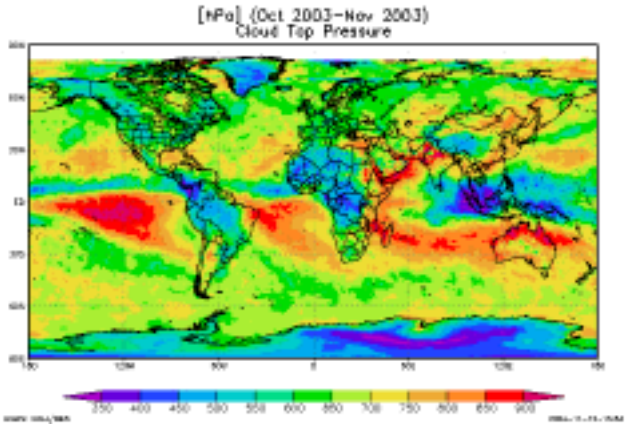


**Figure 9.** Cloud top pressure for MODIS observations, October and November 2003;

## 4. SUMMARY AND CONCLUSIONS

In our presentation, we show global cloud occurrence frequency and cloud top height distributions derived from the GLAS observations that comprise part of the standard GLAS cloud data product. These results establish the effectiveness of using GLAS cloud products for climatological studies. We demonstrate that spaceborne lidar is a sensitive tool for making routine long term global cloud observations. As an active instrument, It. has advantages over radiometers in determining the altitude of tenuous high clouds and detecting occurrences of multiple layers We show that lidar can complement and validate cloud radiometer observations. We find that continuous long term observations by GLAS can provide valuable information for determining cloud cover changes and trends. These early results from GLAS suggest that future observations by GLAS and other spaceborne lidars (for example, Cloud-Aerosol Lidar with Orthogonal Polarization (CALIOP) scheduled for 2005 launch), will be a vital component in the effort to measure changes and trends global cloud cover.

## 5. ACKNOWLEDGEMENT

MODIS cloud distribution and cloud top height maps, Figures 8 and 9.
The data used in this study were acquired as part of the NASA's Earth Science Enterprise. The algorithms were developed by the MODIS Science Teams. The data were processed by the MODIS Adaptive Processing System (MODAPS) and Goddard Distributed Active Archive Center (DAAC), and are archived and distributed by the Goddard DAAC.

## 6. REFERENCES

Palm, S. P., W. Hart, D. L. Hlavka, E. J. Welton, A. Mahesh, and J. D. Spinhirne, GLAS Atmospheric Data Products, Geoscience Laser Altimeter System (GLAS) algorithm theoretical basis document, Version 4.2, *Goddard Space Flight Center*, 137 pp., 2002 [Available online at eospso.gsfc.nasa.gov/eos_homepage/for_scientists/atbd/docs/GLAS/ATBD-GLAS-01.pdf].

Wylie, P. W., W. P. Menzel, H. M. Woolf, and K. I. Strabala; 1994; Four Years of Global Cirrus Cloud Statistics Using HIRS; J. of Climate; Vol. 7,No. 12, p 1972-1986